PNAS

Supporting Information for

A high-fat diet promotes cancer progression by inducing gut microbiota-mediated leucine production and PMN-MDSC differentiation

Jiewen Chen[a,b,c,1], Xiyuan Liu[d,1], Yi Zou[d], Junli Gong[d,e], Zhenhuang Ge[d], Xiaorong Lin[f], Wei Zhang[g], Hongyan Huang[h], Jianli Zhao[a], Phei Er Saw[a], Yongjun Lu[d,2], Hai Hu[a,g,2], Erwei Song[a,b,2]

[a]Guangdong Provincial Key Laboratory of Malignant Tumor Epigenetics and Gene Regulation, Guangdong-Hong Kong Joint Laboratory for RNA Medicine, Sun Yat-sen Memorial Hospital, Sun Yat-sen University, Guangzhou 510120, China; [b]Breast Tumor Center, Sun Yat-sen Memorial Hospital, Sun Yat-sen University, Guangzhou 510120, China; [c]Department of Breast Medicine, Affiliated Foshan Maternity and Child Healthcare Hospital, Southern Medical University, Foshan 528000, Guangdong, China; [d]Run-ze Laboratory for Gastrointestinal Microbiome Study, School of Life Sciences, Sun Yat-sen University, Guangzhou 510275, China; [e]Present address: Department of Colorectal Surgery and Run-ze Laboratory for Gastrointestinal Microbiome Study, the Sixth Affiliated Hospital of Sun Yat-sen University, Guangzhou, 510655, China; [f]Diagnosis and Treatment Center of Breast Diseases, Shantou Central Hospital, Shantou 515000, China; [g]Department of Oncology, Sun Yat-sen Memorial Hospital, Sun Yat-sen University, Guangzhou 510120, China; and [h]Department of Breast Surgery, Zhujiang Hospital, Southern Medical University, Guangzhou 510282, China

[1]Jiewen Chen and Xiyuan Liu contributed equally to this work.

[2]To whom correspondence may be addressed. Email: songew@mail.sysu.edu.cn, huhai@mail.sysu.edu.cn or luyj@mail.sysu.edu.cn

This PDF file includes:

Sumpplementary Materials and Methods

Figures and Figure legends S1 to S7

Tables S3 to S5

Supplementary Materials and Methods

Patients and tissue samples.

The follow-up information of 5031 female patients with breast cancer was acquired from the follow-up system at the Breast Tumor Center, Sun Yat-sen Memorial Hospital, Sun Yat-sen University (Guangzhou, China), between 2001 and 2020. Patients were followed up for 2–144 months (median follow-up, 36 months). Fecal and breast cancer samples for gut microbial and leucine examination were collected from 61 female patients with breast cancer. Information regarding the 61 patients is presented in Table S1. Serum and breast cancer tissue samples from 163 female patients were obtained for further leucine and MDSCs analyses. Serum samples were obtained from 18 female patients with benign breast tumors for leucine examination. Information on the 181 patients is shown in Table S2. The cutoff of overweight (BMI 24-28) and obesity (BMI>28) of Chinese patients was defined according to Criteria of weight for adults enacted by Chinese Center for Disease Control and Prevention. Informed consent was obtained from all the enrolled patients. This study was approved and monitored by Sun Yat-sen Memorial Hospital's Institutional Review Board (Approval No. 2021-59).

16s rRNA sequencing.

Human and mouse fecal samples were collected at the experimental endpoint, promptly frozen in liquid nitrogen, and then stored at -80 °C. Total DNA was extracted from the frozen fecal samples using the QIAamp® Fast DNA Stool Mini Kit (Qiagen, Germany). For mouse fecal samples, the variable V3-V4 regions of the 16S rDNA were PCR-amplified and sequenced on an Illumina MiSeq PE250 platform. In the case of human fecal samples, full-length 16S rDNA was PCR-amplified and sequenced using a Pacific Biosciences (PacBio) Single-Molecule Real-Time sequencing platform. The sequencing procedures followed standard protocols and were conducted at Biomarker Technologies Co., Ltd. (Beijing, China). Raw sequences have been deposited in the NCBI Sequence Read Archive database (http://www.ncbi.nlm.nih.gov/sra) under the accession numbers ranging from SRR18912085 to SRR18912170.

Primary cell acquisition and flow cytometry.

Primary circulating immune cells were isolated through red blood cell lysis, while primary tumor cells were obtained via mechanical dissociation and collagenase digestion. Bone marrow cells were acquired through red blood cell lysis as well. For flow cytometry analysis, primary cells were stained with antibodies for 30 minutes at 4 °C. Flow cytometry procedures were carried out using a FACS Verse instrument (BD Bioscience, CA, USA), and the resulting data were analyzed using Kaluza 2.1 software (Beckman Coulter, CA, USA). The specific antibodies used are detailed in Table S5.

Animal models and treatments.

Female FVB/N-Tg(MMTV-PyMT) 634Mul/J transgenic and wild-type FVB mice were purchased from the Model Animal Research Center of Nanjing University (http://www.nicemice.cn/). Four-week-old female C57BL/6 and BALB/c mice were purchased from Gem Pharmatech (Shanghai, China). Following standard operational procedures, all mice were housed in a specific pathogen-free grade room at the Forevergen Laboratory Animal Center (Guangzhou, China).

For the Normal-fat diet (NFD) and high-fat diet (HFD) groups, mice were fed either an NFD or HFD (D12492, Rodent Diet with 60 kcal% Fat, Research Diets, Inc.). In the case of mice-derived fecal microbiota transplantation (FMT), fecal samples were collected from wild-type FVB or C57BL/6 mice that had been fed a high-fat diet. These samples were then diluted in sterile phosphate-buffered saline (PBS) at a concentration of 2 mg/1 mL. The suspension was incubated at room temperature for 2 minutes. Four-week-old mice received 200 μL of the fecal supernatant through oral gavage twice weekly until dissection. The control group was administered 200 μL of PBS.

For antibiotic treatment, four-week-old HFD or HDFMT mice were treated with ampicillin (1 g/L), vancomycin (0.5 g/L), neomycin (1 g/L), and metronidazole (1 g/L) (Sigma-Aldrich, St. Louis, MO, USA), or placebo in drinking water as a control.

For leucine treatment, four-week-old mice were provided with 200 μL Leucine (10 mg/mL, Sigma-Aldrich, St. Louis, MO) by oral gavage twice weekly. The control group was provided with 200 μL PBS.

Anti-Gr1 was used to deplete MDSCs to investigate the role of MDSCs in high-fat-diet treatment and fecal microbiota transplantation. Four-week-old mice were intraperitoneally injected with 100 mg of neutralizing anti-Gr1 antibody (BE0075, BioxCell, USA) twice weekly until dissection. The control group received 100 mg anti-isotype IgG.

For the *Desulfovibrio desulfuricans* colonization model, a strain of *D. desulfuricans* was generously provided by the Guangdong Institute of Microbiology. *D. desulfuricans* was anaerobically cultured in ATCC Medium 1249 at 37 °C for 2-3 days. The strain was subsequently harvested by centrifugation at 6000 g for 5 minutes, washed twice with normal saline, and resuspended in sterile normal saline containing 30% glycerol, resulting in a final concentration of 10^6 CFU mL^{-1}. Subsequently, 200 μL of the bacterial solution prepared above was administered to germ-free mice through oral gavage twice weekly. Germ-free BALB/c mice were raised in a germ-free environment, fed a normal-fat diet, and administered with either 200 μL of bacterial strain preservation solution (Control) or *D. desulfuricans* (*Dd*) via oral gavage twice weekly until dissection. Two weeks after the initiation of *D. desulfuricans* gavage, mice were inoculated with 100 μL (1×10^6 cells) of 4T1 mouse breast cancer cells on the second right mammary fat pad.

For the Everolimus treatment, 4-week-old mice were administered Everolimus (Selleckchem, TX, USA, 1 mg/kg) or a solvent (0.5%CMC-Na) as a control twice weekly until dissection.

For patient-derived fecal microbiota transplantation, fecal samples were collected from three female normal-weight (lean cases) and three obese donors (obese cases). Fecal samples from the same group were mixed (weight=1:1:1), suspended with, and stored at -80 °C. Four-week-old mice were first treated with ampicillin (1 g/L), vancomycin (0.5 g/L), neomycin (1 g/L), and metronidazole (1 g/L) for 1 week and then supplied with 200 μL fecal supernatant by oral gavage once a week until dissection. Mice with normal-weight donor-derived FMT were fed 200 μL PBS

and 200 μL leucine (10 mg/mL). Mice with obese donor-derived FMT were fed 200 μL PBS or 200 μL Nimesulide (20 mg/kg, Sigma). The control group was supplied with the 200 μL medium.

Tumor growth and tissue collection.

The mice were weighed weekly throughout the experiment. The mammary tumor width and length were measured using a digital caliper, and accurate volume calculations were obtained using the following formula: volume =1/2 ($Width^2$ × Length). At the experimental endpoint, the mice were euthanized with 4% pentobarbital, and their eyeballs were removed to obtain blood. Blood was collected in an EDTA anticoagulation tube to obtain whole blood and in an Eppendorf tube to obtain serum. The Eppendorf was held at room temperature for 30 min, then centrifuged at 2000 rpm for 5 min to remove the clot, and the supernatant was restored at -80 °C. Mammary tumors were excised and weighed. Then, the tumors were stored in the RNA Keeper Tissue Stabilizer (Vazyme Co. Ltd., Nanjing, China) and 10% neutral formalin separately or snap-frozen in liquid nitrogen and stored at −80 °C. The limbs were removed and kept in RPMI-1640 for further experiments.

Magnetic separation of CD3e+ T lymphocytes and Gr-1$^+$ MDSCs.

For CD3e$^+$ T lymphocyte sorting, spleens from mice were obtained and crushed into pieces. The tissue suspension was filtered through a strainer, and erythrocytes were lysed using erythrocyte lysis buffer. After washing twice with separation buffer, cells were orderly incubated with antiCD3ε biotin-conjugated antibody (10 μL per 10^7 total cells) and biotin-microbeads (20 μL per 10^7 total cells) at 4 °C for 10 min for further magnetic sorting. For MDSCs sorting, primary tumor cells were obtained by mechanical dissociation and collagenase digestion. Then, they were orderly incubated with anti-Gr-1 biotin-conjugated antibody (10 μL per 10^7 total cells) and biotin-microbeads (20 μL per 10^7 total cells) at 4 °C for 10 min for further magnetic sorting. After the magnetic labeling, the isolation was performed by immunomagnetic separation using LS columns (130-042-401, Miltenyi Biotec) and the midi-MACS system (Miltenyi Biotec) following the manufacturer's instructions.

Metabolomics analysis.

All reference metabolites were purchased from Sigma-Aldrich (St. Louis, MO, USA), Nu-Chek Prep (Elysian, MN, USA), and Santa Cruz Biotechnology (Dallas, TX, USA). For microbes-host co-metabolites analysis, fecal samples were collected at the experimental endpoint, snap-frozen in liquid nitrogen, and stored at -80 °C until analysis. The sample preparation and derivation methods were based on a procedure previously published by Zheng et al. with modifications. Notably, all prepared samples were analyzed within 48 h of extraction and derivatization. Gas chromatography coupled with a time-of-flight mass spectrometry (GC-TOFMS) system (Pegasus HT, Leco Corp., St. Joseph, MO, USA) operated in electron ionization (EI) mode was used to quantify the metabolites at Metabo-Profile Biotechnology (Shanghai) Co., Ltd. (Shanghai, China). For the serum Branched-chain amino acid (BCAA) examination, 900 μL precipitation solution was added to a 1.5 mL centrifuge tube on ice, then 100 μL L-Norvaline (10 μg/mL) was added and vibrated for seconds, followed by the addition of 10 μL of the sample into the extraction solution (5 mL methanol + 15 mL acetonitrile + 100 μL L-Norvaline). Furthermore, 1000 μL LC/MS grade water was added to resuspend the sample before the Liquid chromatography-mass spectrometry (LC-MS/MS) analysis. The resuspended sample was transferred to an insert, the cap was covered, the vial was knocked to shake out the bubbles at the bottom of the vial insert, and then the sample was subjected to LC-MS/MS testing.

Western blot analysis.

Tissue and cellular protein samples were extracted through the ristocetin-induced platelet aggregation buffer. Furthermore, 10% sodium dodecyl (lauryl) sulfate-polyacrylamide gel electrophoresis was used to separate the protein samples (40 μg); they were transferred onto polyvinylidene fluoride membranes, blocked with 5% non-fat milk, incubated with the primary antibody, and incubated with horseradish peroxidase-linked secondary antibodies in sequence. Chemiluminescence was used for visualization. The antibodies are shown in Table S5.

Immunofluorescence assay (IF).

Breast cancer tissues collected from patients were fixed in 10% neutral formalin, embedded in paraffin, and sectioned. Sections for antigen retrieval were incubated with primary antibodies (rabbit monoclonal anti-CD3e and mouse monoclonal anti-CD33) and fluorescence-conjugated secondary antibodies in sequence. DAPI was used for staining. Positive signals were examined using confocal microscopy. The antibodies used in this study are listed in Table S5.

Quantitative reverse transcription PCR (qRT-PCR).

Tissue and cellular RNA were isolated using TRIzol reagent (Invitrogen, USA), as previously reported [1]. Reverse transcriptase and SYBR qPCR kits (Vazyme, Nanjing, China) were used for cDNA acquisition and qRT-PCR.

CarboxyFluoroscein Succinimidyl Ester (CFSE).

Tumor MDSCs were sorted using flow cytometry (lived $CD45^+$ $CD11b^+$ $Gr\text{-}1^+$ cells). Splenic T lymphocytes were sorted using anti-CD3e magnetic beads. The sorted $CD3e^+$ T lymphocytes were collected, centrifuged at 400 × g for 10 min, and resuspended in 1 mL of PBS. Then, the CFSE solution was added and placed at 37 °C for 30 min. Furthermore, 5mL of RPMI-1640 medium (containing 10% FBS) was added and incubated for 5 min at 37 °C. Centrifugation was performed at 400 × g for 5 min, the supernatant was removed, and the complete medium was added. Phytohaemagglutinin (PHA, 10 μg/mL) was added to stimulate $CD3^+$ T lymphocyte proliferation, and selected MDSC cells were added for co-culture (MDSC: T lymphocyte=1:1). After a 96-h culture, the proliferation of $CD3^+$ T lymphocytes was detected using flow cytometry after adding the anti-CD3e antibody.

In vitro MP induction.

The bone marrow cells were collected. MPs were sorted using flow cytometry (lived $lineage^-$ $ckit^+$ $sca\text{-}1^-$ cells). Sorted cells were seeded in 96-well culture plates (10^5 cells/well) and cultured in RPMI-1640 medium containing 10% FBS. For serum application, 10 μL serum was added into cells, with or without Everolimus application (100 nM/well). For amino acid application, 50 μg/mL, 100 μg/mL, and 150 μg/mL leucine, 50μg/mL isoleucine and 20μg/mL valine were added into

cells. After a 6-day culture, the cells were collected, and the proportion of MDSCs was detected using flow cytometry.

Sestrin2 knockdown in MPs.

Small interfering RNA was used to transiently suppress the expression of sestrin2 in MPs. Briefly, MP cells sorted from the bone marrow were incubated with complexes of lipo3000/siSestrin2-1 or lipo3000/siSestrin2-2 for 12 h. Following this incubation, the cells were rinsed with PBS and subsequently cultured in a medium supplemented with FBS for another 48 h.

Figure S1

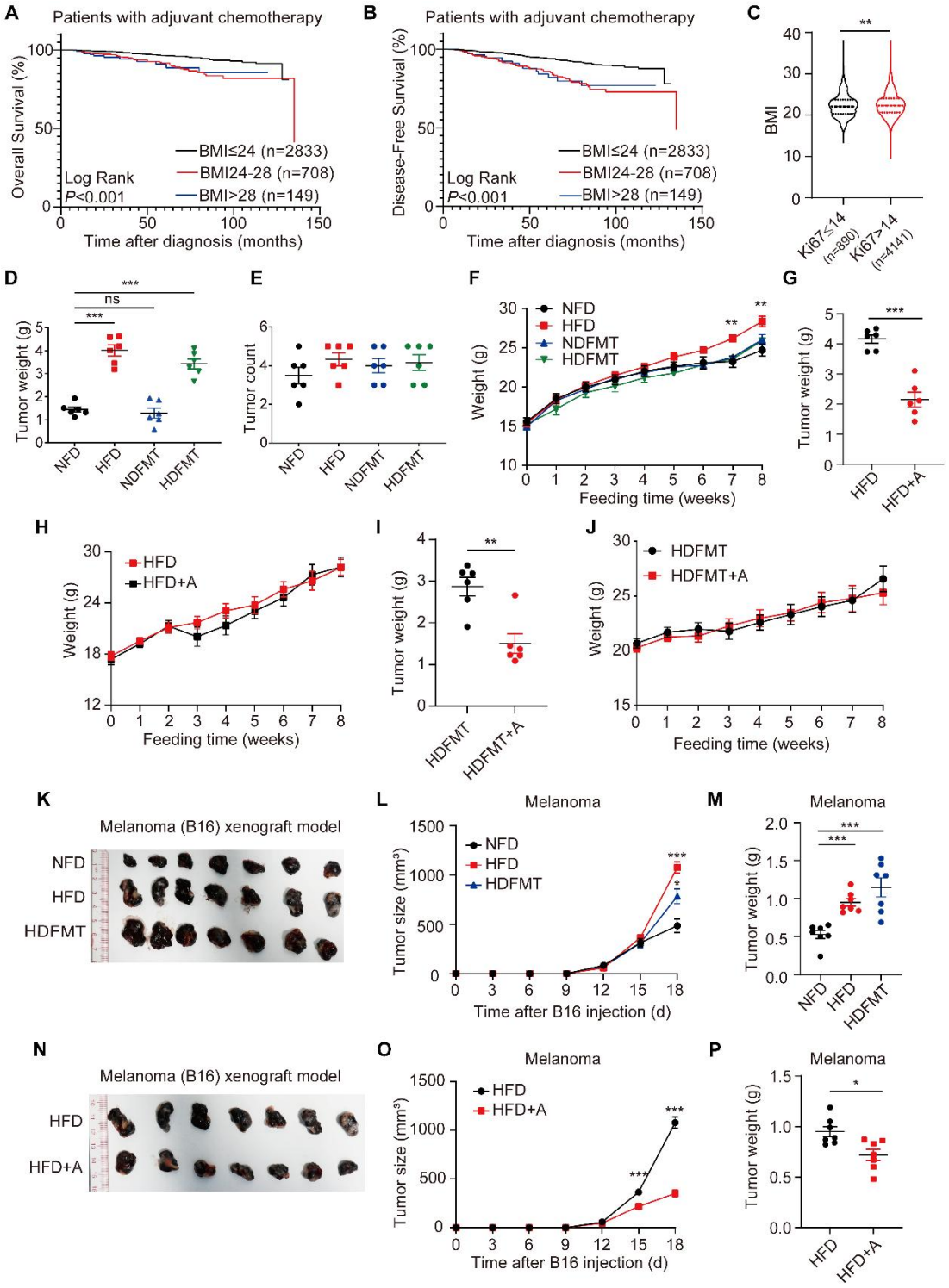

Fig. S1. HFD promotes tumor progression through dysbiosis of gut microbiota. (*A*) KM curve of OS for breast cancer patients who were treated with adjuvant chemotherapy with BMI

≤24 (n=2833), 24–28 (n=708), and >28 (n=149). (*B*) KM curve of DFS for breast cancer patients who were treated with adjuvant chemotherapy with BMI ≤24 (n=2833), 24–28 (n=708), and >28 (n=149). (*C*) Violin plot represents the BMI of breast cancer patients with Ki67 ≤14 (n=890) and >14 (n=4141). (*D*) Dot plot represents the weight of breast cancer tissues from MMTV/PyMT mice with NFD, HFD and HDFMT (n=6 per group). (*E*) Dot plot represents the count of breast cancer tissues from MMTV/PyMT mice with NFD, HFD, NDFMT and HDFMT (n=6 per group). (*F*) Curve represents the body weight of MMTV/PyMT mice with NFD, HFD, NDFMT and HDFMT (n=6 per group). (*G*) Dot plot represents the weight of breast cancer tissues from MMTV/PyMT mice with HFD and HFD+A (n=6 per group). (*H*) Curve represents the body weight of MMTV/PyMT mice with HFD and HFD+A (n=6 per group). (*I*) Dot plot represents the weight of breast cancer tissues from MMTV/PyMT mice with HDFMT and HDFMT+A (n=6 per group). (*J*) Curve represents the body weight of MMTV/PyMT mice with HDFMT and HDFMT+A (n=6 per group). (*K*) Image of melanoma from C57/BL6 mice with NFD, HFD and HDFMT (n=7 per group). (*L*) Tumor growth curve of melanoma from C57/BL6 mice with NFD, HFD and HDFMT (n=7 per group). (*M*) Dot plot represents the weight of melanoma from C57/BL6 mice with NFD, HFD and HDFMT (n=7 per group). *(N)* Image of melanoma from C57/BL6 mice with HFD and HFD+A (n=7 per group). (*O*) Tumor growth curve of melanoma from C57/BL6 mice with HFD and HFD+A (n=7 per group). (*P*) Dot plot represents the weight of melanoma from C57/BL6 mice with HFD and HFD+A (n=7 per group). Data are presented as mean ± SEM, *P* values are calculated by Student's t test or Tukey's post-hoc test. **P* <0.05; ***P* <0.01; ****P* <0.001.

Figure S2

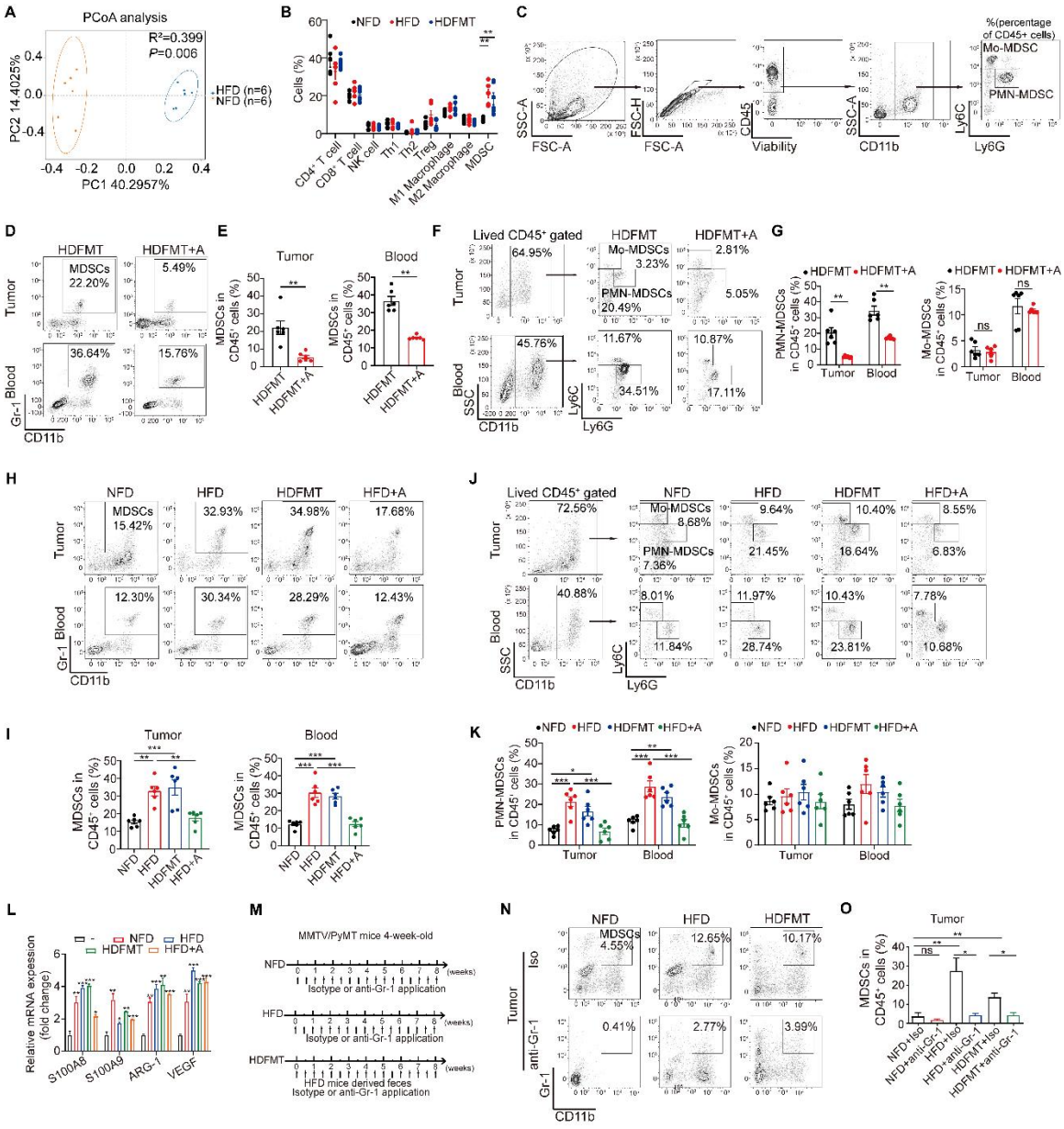

Fig. S2. HFD-mediated gut microbiota dysbiosis promotes tumor progression via PMN-MDSCs. (*A*) PCoA plot with Bray–Curtis dissimilarity of fecal microbiota from NFD and HFD groups based on the operational taxonomic unit (OTU) data (n=6 per group). The x- and y-axes are indicated by the first and second coordinates, respectively. (*B*) Dot plot represents the level of immune cell infiltration in breast tumor tissue from NFD, HFD, and HDFMT groups (n=6 per group). (*C*) Flow cytometry gating strategy chart for MDSC subtypes. (*D*) The proportion of MDSCs in the tumor and circulation in the HDFMT and HDFMT+A groups was determined using

flow cytometry (n=6 per group). *(E)* Scatter plots represent the proportion of MDSCs in the tumor (left) and circulation (right) in the HDFMT and HDFMT+A groups (n=6 per group). *(F)* The proportion of PMN-MDSCs and Mo-MDSCs in breast tumor tissue and circulation from the HDFMT and HDFMT+A groups was determined using flow cytometry (n=6 per group). *(G)* Scatter plots represent the proportion of PMN-MDSCs (left) and Mo-MDSCs (right) in breast tumor tissue and circulation from the HDFMT and HDFMT+A groups (n=6 per group). (*H*) Proportion of MDSCs in melanoma tissue and circulation from NFD, HFD, HDFMT and HFD+A groups was determined by flow cytometry (n=6 per group). (*I*) Scatter plots represen the proportion of MDSCs in melanoma tissue (left) and circulation (right) from NFD, HFD, HDFMT and HFD+A groups (n=6 per group). *(J)* Proportion of PMN-MDSCs and Mo-MDSCs in melanoma tissue and circulation from NFD, HFD, HDFMT and HFD+A groups was determined by flow cytometry (n=6 per group). *(K)* Scatter plots represent the proportion of PMN-MDSCs (left) and Mo-MDSCs (right) in melanoma tissue and circulation from the NFD, HFD, HDFMT and HFD+A groups (n=6 per group). (*L*) mRNA level of *S100A8*, *S100A9*, *ARG-1*, and VEGF from sorted MDSCs from NFD, HFD, HDFMT and HFD+A melanoma tissue was determined by qRT-PCR. All values are means ± SEM, n=3 independent experiments of tumoral MDSCs from background mice, NFD, HFD and HDFMT mice. (*M*)Instruction of neutralizing anti-Gr-1 antibody application model. (*N*) Efficacy of MDSCs depletion as determined by flow cytometry (n=5 per group). (*O*) A scatter plot represents the proportion of MDSCs in breast cancer tissue from NFD, HFD, and HDFMT groups with or without neutralizing anti-Gr-1 antibody application (n=5 per group). Data are presented as mean ± SEM, *P* values are calculated by Student's t test or Tukey's post-hoc test. **P* <0.05; ***P* <0.01; ****P* <0.001.

Figure S3

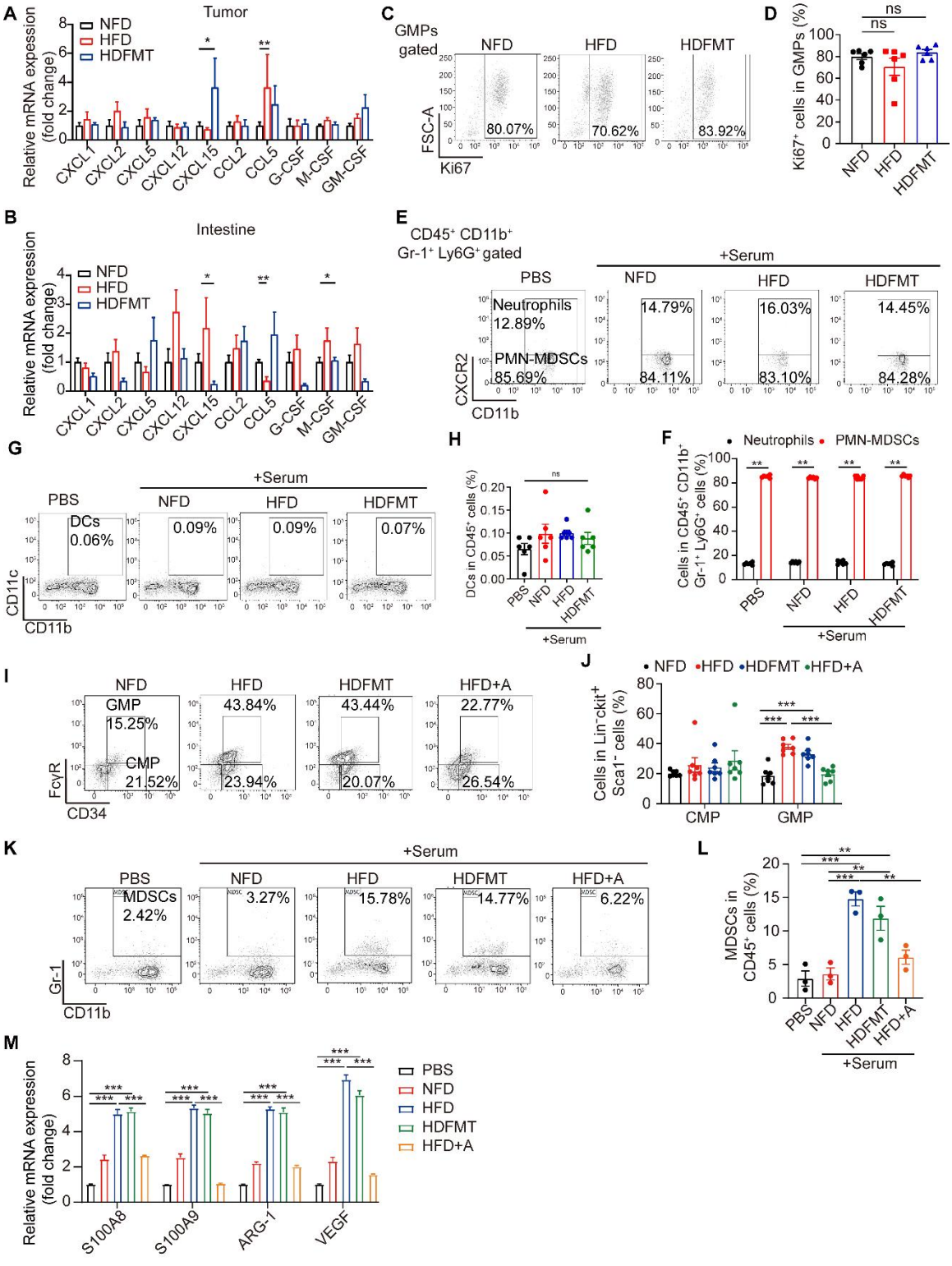
A
Tumor
NFD
HFD
HDFMT
Relative mRNA expression (fold change)
CXCL1
CXCL2
CXCL5
CXCL12
CXCL15
CCL2
CCL5
G-CSF
M-CSF
GM-CSF
B
Intestine
C
GMPs gated
NFD
HFD
HDFMT
80.07%
70.62%
83.92%
FSC-A
Ki67
D
Ki67+ cells in GMPs (%)
ns
E
CD45+ CD11b+ Gr-1+ Ly6G+ gated
+Serum
PBS
Neutrophils 12.89%
PMN-MDSCs 85.69%
14.79%
84.11%
16.03%
83.10%
14.45%
84.28%
CXCR2
CD11b
F
Neutrophils
PMN-MDSCs
Cells in CD45+ CD11b+ Gr-1+ Ly6G+ cells (%)
G
DCs 0.06%
0.09%
0.09%
0.07%
CD11c
H
DCs in CD45+ cells (%)
I
GMP 15.25%
CMP 21.52%
43.84%
23.94%
43.44%
20.07%
22.77%
26.54%
FcγR
CD34
J
HFD+A
Cells in Lin-ckit+ Sca1- cells (%)
CMP
GMP
K
MDSCs 2.42%
3.27%
15.78%
14.77%
6.22%
Gr-1
L
MDSCs in CD45+ cells (%)
M
S100A8
S100A9
ARG-1
VEGF

Fig. S3. HFD-mediated microbiota dysbiosis triggers PMN-MDSCs production. (*A*) mRNA level of *CXCL* and *CSF* in breast cancer tissue from NFD, HFD, and HDFMT groups was determined by qRT-PCR. All values are means ± SEM, n=6 independent experiments of breast cancer tissue from NFD, HFD and HDFMT mice. (*B*) mRNA level of *CXCL* and *CSF* in intestinal tissues from NFD, HFD, and HDFMT groups was determined by qRT-PCR. All values are means ± SEM, n=6 independent experiments of intestine tissue from NFD, HFD and HDFMT mice. (*C*) Proprotion of Ki67 positive GMPs in the bone marrow of mice with breast tumor burden from NFD, HFD, and HDFMT groups was determined using flow cytometry (n=6 per group). (*D*) A scatter plot represents proportion of Ki67 positive GMPs in the bone marrow of mice with breast tumor burden from NFD, HFD, and HDFMT groups. (*E*) MPs were treated with PBS and sera from NFD, HFD, and HDFMT mice (breast cancer-burdened). The proportion of $CXCR2^{high}$ or $CXCR2^{low}$ cells in $CD45^+$ $CD11b^+$ $Gr\text{-}1^+$ $Ly6G^+$ cells was determined by flow cytometry. (n=6 per group). (*F*) A scatter plot represents proportion of generated $CXCR2^{high}$ or $CXCR2^{low}$ cells in $CD45^+$ $CD11b^+$ $Gr\text{-}1^+$ $Ly6G^+$ cells. (*G*) MPs were treated with PBS and sera from NFD, HFD, and HDFMT mice (breast cancer-burdened). The proportion of generated DCs was determined by flow cytometry. (n=6 per group). (*H*) A scatter plot represents proportion of generated DCs. (*I*) The proportion of CMPs and GMPs in the bone marrow of mice with melanoma burdened from NFD, HFD, HDFMT, and HFD+A groups were determined by flow cytometry (n=6 per group). (*J*) A scatter plot represents the proportion of CMPs and GMPs in the bone marrow from mice with melanoma burdened from NFD, HFD, HDFMT, and HFD+A groups (n=6 per group). (*K*) MPs were treated with PBS and sera from NFD, HFD, HDFMT, and HFD+A mice (melanoma burdened). Proportion of MDSCs was determined by flow cytometry. n=6 independent experiments of PBS, serum from NFD, HFD, HDFMT and HFD+A mice. (*L*) A scatter plot represents the proportion of generated MDSCs. n=6 independent experiments of PBS, serum from NFD, HFD, HDFMT and HFD+A mice. (*M*) mRNA level of *S100A8*, *S100A9*, *ARG-1*, and *VEGF* of MP cells treated with PBS and sera from NFD, HFD, HDFMT, and HFD+A mice (melanoma burdened) was determined by qRT-PCR. n=3 independent experiments of PBS, serum from NFD, HFD, HDFMT, and HFD+A mice

(melanoma burdened). Data are presented as mean ± SEM. *P* values are calculated by Student's t test or Tukey's post-hoc test. **P* <0.05; ***P* <0.01; ****P* <0.001.

Figure S4

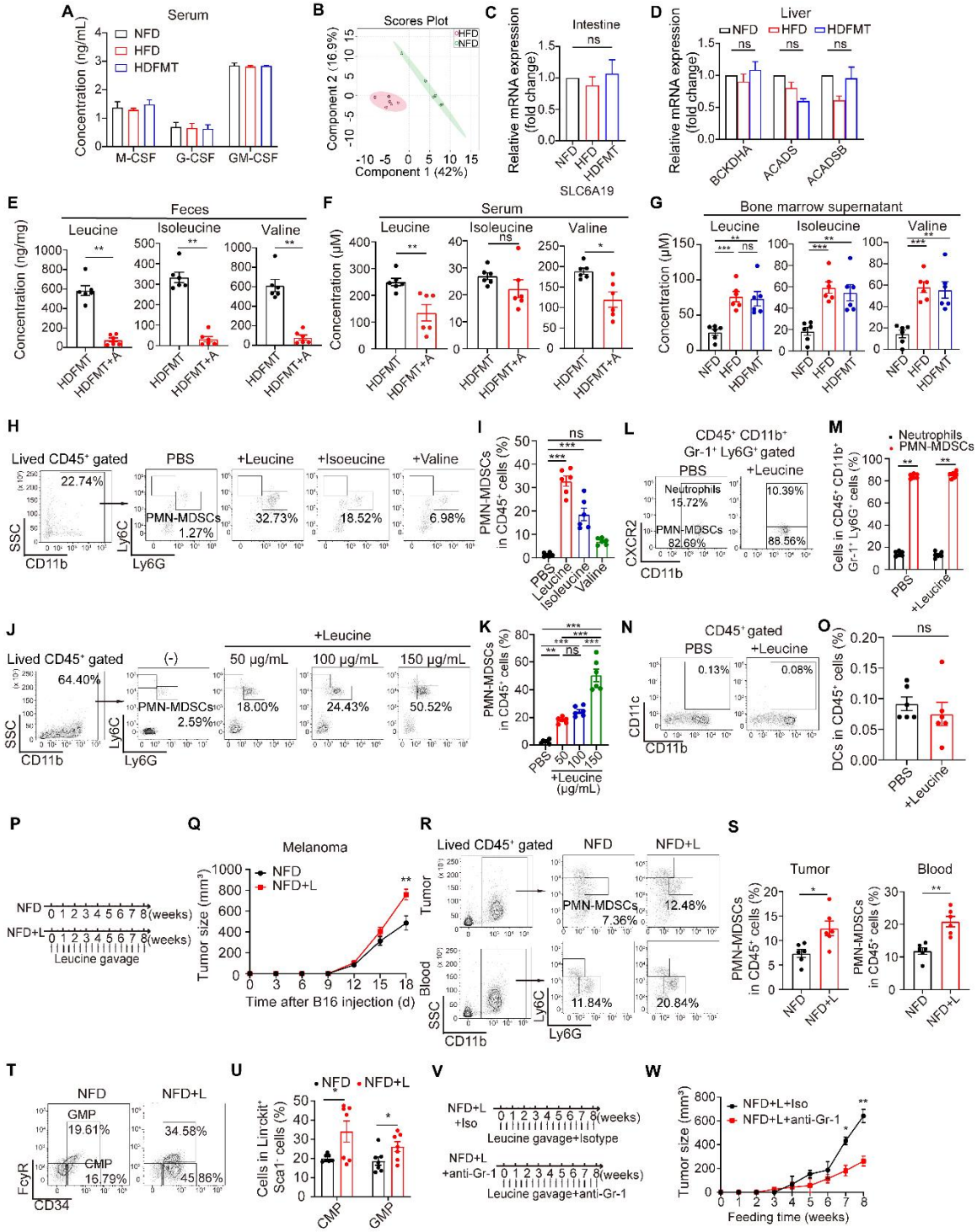

Fig. S4. HFD-mediated dominant microbes produce leucine to enhance PMN-MDSCs differentiation and tumor progression. (*A*) Levels of serum M-CSF, G-CSF, and GM-CSF from NFD, HFD, and HDFMT mice were determined by ELISA (n=5 per group). (*B*) PLS-DA plot of

fecal metabolites from NFD and HFD groups. Each individual was represented by a dot (n=6 per group). (*C*) Expression of *SCL6A19* in ileum tissue from NFD, HFD, and HDFMT groups were determined by qRT-PCR. Three independent experiments were conducted. Data are presented as mean ± SEM. (*D*) Expression of *BCKDHA*, *ACADS*, and *ACADSB*, respectively, in liver tissue from NFD, HFD, and HDFMT groups. Three independent experiments were conducted. Data are presented as mean ± SEM. *(E)* Concentration of leucine, isoleucine, and valine in feces of HDFMT, and HDFMT+A groups (n=6 per group). *(F)* The concentration of leucine, isoleucine, and valine in the serum of HDFMT, and HDFMT+A groups (n=6 per group). *(G)* The concentration of leucine, isoleucine, and valine in the bone marrow supernatant of NFD, HFD, and HDFMT groups (n=6 per group). (*H*) MPs were sorted by flow cytometry and treated with PBS, leucine, isoleucine, and valine for 6 days. The proportion of PMN-MDSCs differentiated from treated MPs was determined by flow cytometry. n=6 independent experiments of PBS, leucine, isoleucine, and valine. (*I*) A scatter plot represents the proportion of generated PMN-MDSCs from MPs treated with PBS, leucine, isoleucine, and valine. n=6 independent experiments of PBS, leucine, isoleucine, and valine. (*J*) MPs were sorted by flow cytometry and treated with PBS and 50, 100, and 150 μg/mL leucine for 6 days. The proportion of PMN-MDSCs differentiated from treated MPs was determined by flow cytometry. n=6 independent experiments of PBS, and 50, 100, and 150 μg/mL leucine. (*K*) A scatter plot represents the proportion of generated PMN-MDSCs from MPs treated with PBS and 50, 100, and 150 μg/mL leucine. n=6 independent experiments of PBS, and 50, 100, and 150 μg/mL leucine. (*L*) MPs were treated with PBS and 100 μg/mL leucine. The proportion of $CXCR2^{high}$ or $CXCR2^{low}$ cells in $CD45^+$ $CD11b^+$ $Gr\text{-}1^+$ $Ly6G^+$ cells was determined by flow cytometry (n=6 per group). (*M*) A scatter plot represents proportion of generated $CXCR2^{high}$ or $CXCR2^{low}$ cells in $CD45^+$ $CD11b^+$ $Gr\text{-}1^+$ $Ly6G^+$ cells. (*N*) MPs were treated with PBS and 100 μg/mL leucine. The proportion of generated DCs was determined by flow cytometry. (n=6 per group). (*O*) A scatter plot represents proportion of generated DCs. (*P*) Experimental procedure.4-week-old MMTV/PyMT mice were fed an NFD with PBS or leucine gavage (twice a week). (*Q*) Growth curve of melanoma from NFD and NFD+L groups (n=6 per group). (*R*) Proportion of PMN-MDSCs in melanoma tissue and circulation in the NFD and NFD+L groups was determined

by flow cytometry (n=6 per group). (*S*) Scatter plots represent the proportion of PMN-MDSCs in melanoma tissue (left) and circulation (right) from melanoma-burdened mice in NFD and NFD+L groups (n=6 per group). (*T*) Proportion of CMPs and GMPs cells in bone marrow from melanoma-burdened mice from NFD and NFD+L groups was determined by flow cytometry (n=6 per group). (*U*) A scatter plot represents the proportion of CMPs and GMPs in the bone marrow of mice with melanoma burden from NFD and NFD+L groups (n=6 per group). (*V*) Experimental procedure.4-week-old MMTV/PyMT mice were respectively treated with leucine gavage + anti-isotype injection, and leucine gavage + anti-Gr-1 antibody injection (twice a week). (*W*) Growth curve of breast tumors from NFD+L groups with isotype (n=5) or neutralizing anti-Gr-1 antibody treatment (n=6). Data are presented as mean ± SEM. *P* values are calculated by Student's t test or Tukey's post-hoc test. **P* <0.05; ***P* <0.01; ****P* <0.001.

Figure S5

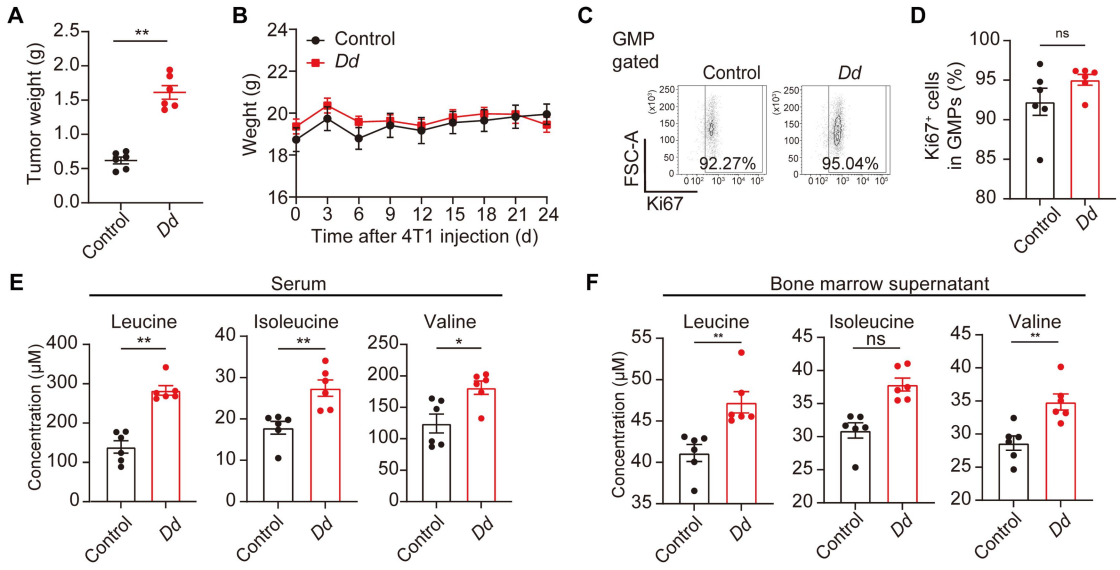

Fig. S5. HFD-mediated enrichment of *Desulfovibrio* augments PMN-MDSCs production and cancer progression through leucine production. *(A)* A dot plot represents the weight of breast cancer tissues from 4T1 tumor bering mice with bacterial strain preservation solution (control) and *Dd* gavage (n=6 per group). *(B)* Curve represents the body weight of 4T1 tumor bearing mice with bacterial strain preservation solution (control) and *Dd* gavage (n=6 per group). (C) Proportion of Ki67 positive GMPs in the bone marrow of 4T1 tumor bearing mice from control and *Dd* gavage groups was determined using flow cytometry. (*D*) A scatter plot represents proportion of Ki67 positive GMPs (n=6 per group). *(E)* Concentration of leucine, isoleucine, and valine in serum of control and *Dd* gavage groups (n=6 per group). *(F)* Concentration of leucine, isoleucine, and valine in bone marrow supernatant of control and *Dd* gavage groups (n=6 per group). Data are presented as mean ± SEM, *P* values are calculated by Student's t test. **P* <0.05; ***P* <0.01; ****P* <0.001.

Figure S6

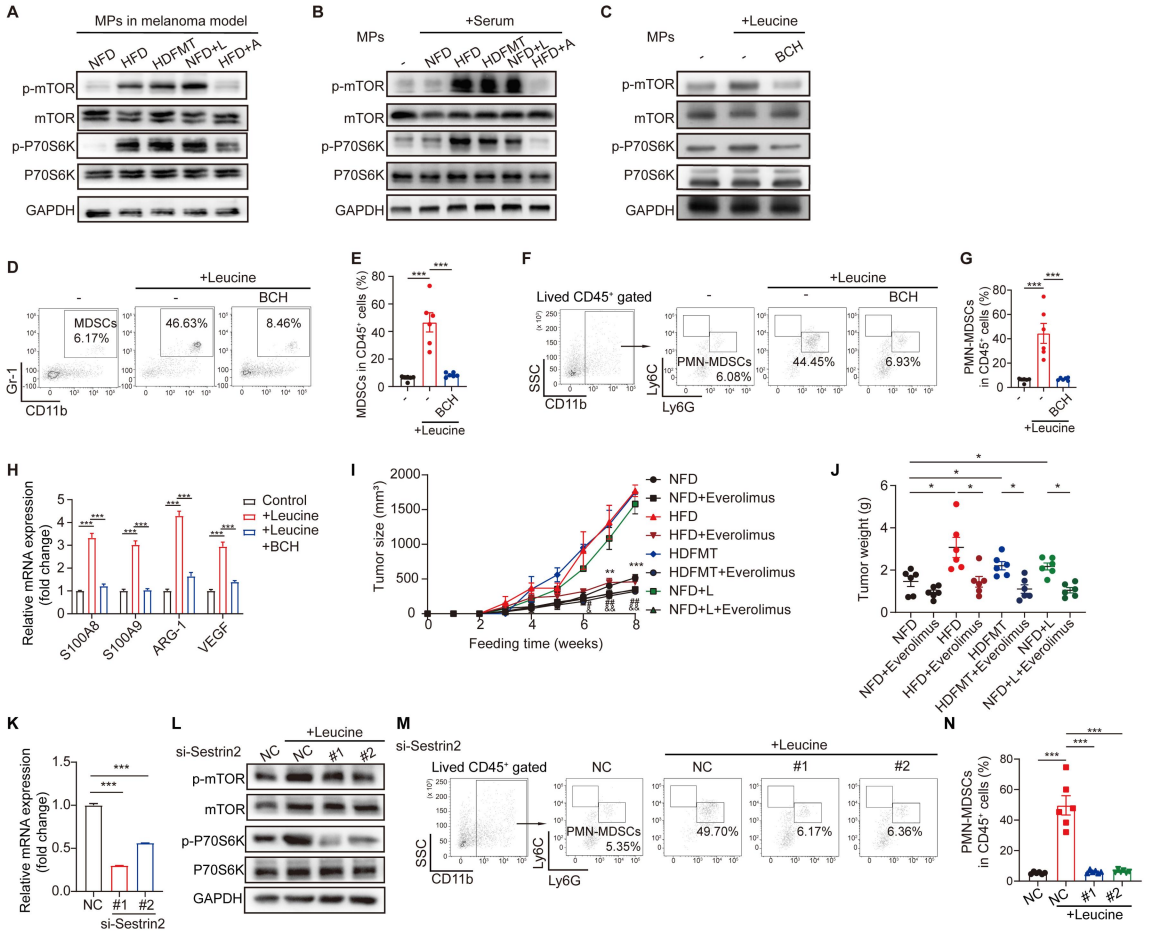

Fig. S6. Leucine triggers MP differentiation towards PMN-MDSCs by activating the mTORC1 signaling pathway. (*A*) Western blotting analysis of MPs from melanoma-bearing mice from NFD, HFD, HDFMT, NFD+L, and HFD+A groups. Target proteins were mTOR, phospho-mTOR, P70S6K, phospho-P70S6K, and GAPDH. A graph represents experimental triplicates. (*B*) Western blotting analysis of MPs treated with PBS, NFD-serum, HFD-serum, HDFMT-serum, NFD+L-serum, and HFD+A-serum. A graph represents experimental triplicates. (*C*) Western blotting analysis of MPs treated with PBS or leucine with or without BCH. A graph represents experimental triplicates. (*D*) MPs were sorted by flow cytometry and treated with PBS (n=6) or leucine with (n=6) or without BCH (n=6) for 6 days. Proportion of MDSCs differentiated from treated MPs was determined by flow cytometry. (*E*) A scatter plot represents the proportion of generated MDSCs from MPs treated with PBS (n=6) or leucine with (n=6) or without BCH (n=6).

(F) MPs were sorted by flow cytometry and treated with PBS (n=6) or leucine with (n=6) or without BCH (n=6) for 6 days. Proportion of PMN-MDSCs differentiated from treated MPs was determined by flow cytometry. (*G*) A scatter plot represents the proportion of generated PMN-MDSCs from MPs treated with PBS (n=6) or leucine with (n=6) or without BCH (n=6). (*H*) mRNA level of *S100A8*, *S100A9*, *ARG-1*, and *VEGF* of MP cells treated with PBS or leucine with or without BCH was determined by qRT-PCR. All values are means ± SEM, n=3 independent experiments of PBS or leucine with or without BCH. (*I*) Growth curve of breast tumors from NFD, HFD, HDFMT, and NFD+L groups with or without Everolimus treatment (n=6 per group). (*J*) Dot plot represents the average weight of breast tumors per mice from NFD, HFD, HDFMT, and NFD+L groups with or without Everolimus treatment (n=6 per group). (*K*) Efficacy of sestrin2 knockdown was determined by qRT-PCR. A graph represents means ± SEM of experimental triplicates. (*L*) Western blotting analysis of MPs, respectively, with NC, Sestrin2 knockdown, sestrin2 knockdown plus leucine treatment. Target proteins were mTOR, phospho-mTOR, P70S6K, phospho-P70S6K, and GAPDH. A graph represented experimental triplicates. (*M*) MPs were sorted by flow cytometry, and sestrin2 was silenced in MPs with or without leucine treatment. Treated cells were cultured for 6 days. Proportion of PMN-MDSCs differentiated from treated MPs was determined by flow cytometry (n=6 per group). (*N*) A scatter plot represents the proportion of generated PMN-MDSCs (n=6 per group). Data are presented as mean ± SEM, *P* values are calculated by Student's t test. **P* <0.05; ***P* <0.01; ****P* <0.001.

Figure S7

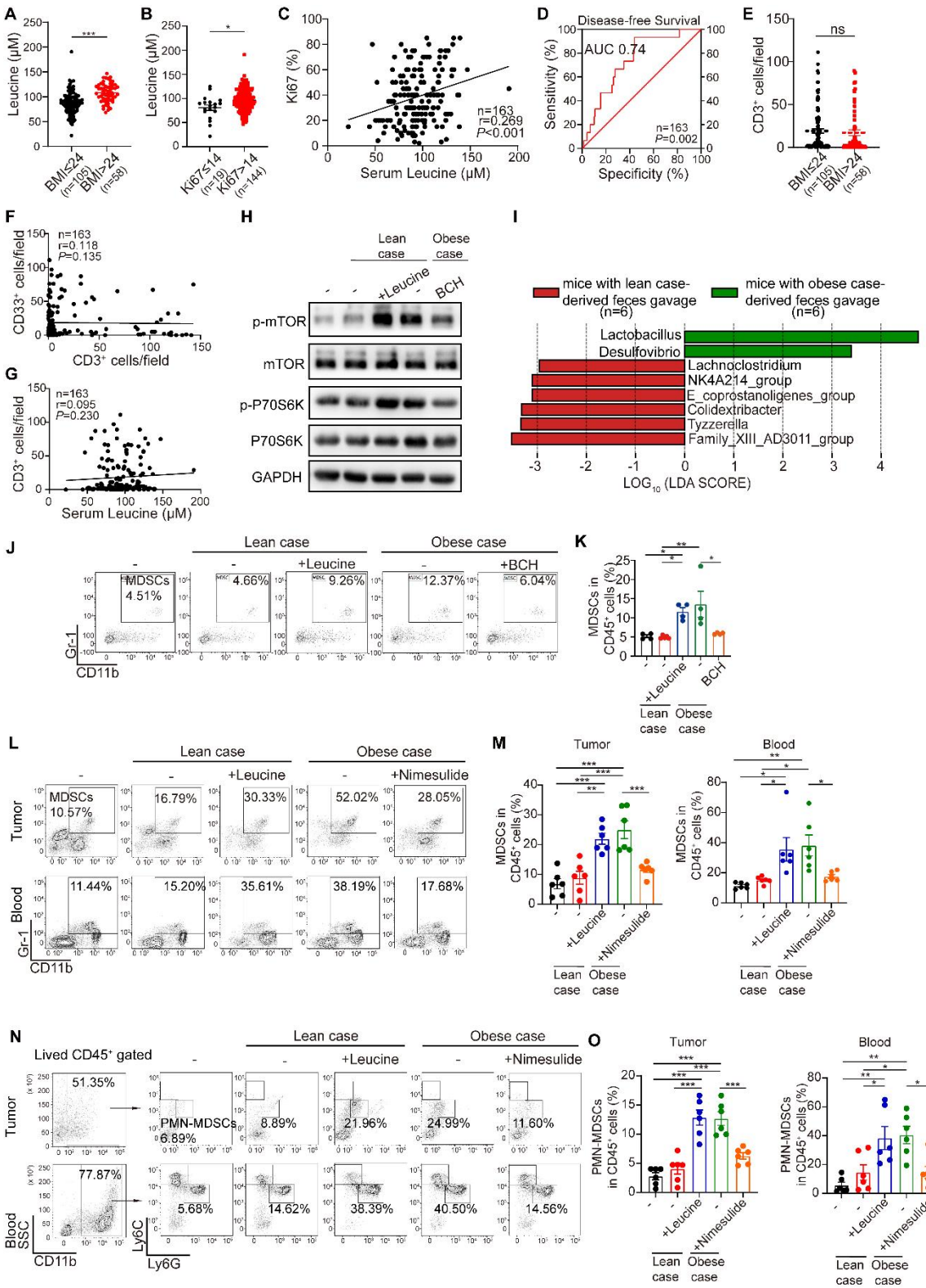
A
Leucine (μM)
BMI≤24 (n=105)
BMI>24 (n=58)
B
Ki67≤14 (n=19)
Ki67>14 (n=144)
C
Ki67 (%)
Serum Leucine (μM)
n=163
r=0.269
P<0.001
D
Disease-free Survival
AUC 0.74
Sensitivity (%)
Specificity (%)
n=163
P=0.002
E
CD3⁺ cells/field
ns
F
CD33⁺ cells/field
CD3⁺ cells/field
n=163
r=0.118
P=0.135
G
CD3⁺ cells/field
Serum Leucine (μM)
n=163
r=0.095
P=0.230
H
Lean case
Obese case
+Leucine
BCH
p-mTOR
mTOR
p-P70S6K
P70S6K
GAPDH
I
mice with lean case-derived feces gavage (n=6)
mice with obese case-derived feces gavage (n=6)
Lactobacillus
Desulfovibrio
Lachnoclostridium
NK4A214_group
E_coprostanoligenes_group
Colidextribacter
Tyzzerella
Family_XIII_AD3011_group
LOG10 (LDA SCORE)
J
Lean case
Obese case
+Leucine
+BCH
MDSCs 4.51%
4.66%
9.26%
12.37%
6.04%
Gr-1
CD11b
K
MDSCs in CD45⁺ cells (%)
+Leucine
BCH
Lean case
Obese case
L
Lean case
Obese case
+Leucine
+Nimesulide
Tumor
Blood
MDSCs 10.57%
16.79%
30.33%
52.02%
28.05%
11.44%
15.20%
35.61%
38.19%
17.68%
Gr-1
CD11b
M
Tumor
Blood
MDSCs in CD45⁺ cells (%)
+Leucine
+Nimesulide
Lean case
Obese case
N
Lived CD45⁺ gated
Lean case
Obese case
+Leucine
+Nimesulide
Tumor
Blood
51.35%
PMN-MDSCs 6.89%
8.89%
21.96%
24.99%
11.60%
77.87%
5.68%
14.62%
38.39%
40.50%
14.56%
SSC
CD11b
Ly6C
Ly6G
O
Tumor
Blood
PMN-MDSCs in CD45⁺ cells (%)
+Leucine
+Nimesulide
Lean case
Obese case

Fig. S7. Serum leucine and HFD-related microbiota are correlated with tumoral MDSCs and advanced clinicopathological status in patients with breast cancer. (*A*) Concentration of serum leucine from malignant breast cancer patients with BMI >24 (n=58) and ≤24 (n=105). (*B*) Concentration of serum leucine from malignant breast cancer patients with Ki67 >14 (n=144) and ≤14 (n=19). (*C*) Spearman's correlation analysis of serum leucine and tumoral Ki67 in breast cancer patients (n=163). (*D*) ROC curve is constructed to estimate the power of serum leucine for predicting the DFS of breast cancer patients. (*E*) A scatter plot represents the number of tumoral T lymphocytes ($CD3^+$ cells) from patients with normal weight (n=105) and overweight/obese (n=58) patients. Total n=163. (*F*) Spearman's correlation analysis of tumoral $CD33^+$ MDSCs and tumoral $CD3^+$ T lymphocytes of patients with breast cancer (n=163). (*G*) Spearman's correlation analysis of serum leucine levels and tumoral $CD3^+$ T lymphocytes of patients with breast cancer (n=163). (*H*) Western blotting analysis of MPs treated with serum from lean donors with or without leucine addition and obese donors with or without BCH addition. Target proteins were mTOR, phospho-mTOR, P70S6K, phospho-P70S6K, and GAPDH. A graph represents of experimental triplicates. *(I)* LEfSe analysis shows statistically differential gut microbes between lean donors-derived FMT and obese donors-derived FMT mice at the genus level. Taxa with a significant LDA threshold value > 2 are shown (n=6 per group). *(J)* MPs were sorted by flow cytometry and treated with serum from lean donors with or without leucine addition and obese donors with or without BCH addition for 6 days. Proportion of MDSCs differentiated from treated MPs was determined by flow cytometry (n=6 per group). (*K*) A scatter plot represents the proportion of MDSCs generated from MPs (n=6 per group). (*L*) Breast cancer-burdened mice were treated with PBS, feces from lean donors, feces from lean donors+leucine, feces from obese donors, and feces from obese donors +Nimesulide, respectively. Proportion of MDSCs in breast cancer tissue and circulation was determined by flow cytometry (n=6 per group). (*M*) Scatter plots represent the proportion of MDSCs in breast cancer tissue (left) and circulation (right). n=6 per group. (*N*) Breast cancer-burdened mice were treated with PBS, feces from lean donors, feces from lean donors +leucine, feces from obese donors, and feces from obese donors +Nimesulide, respectively. Proportion of PMN-MDSCs in breast cancer tissue and circulation was determined

by flow cytometry (n=6 per group). (*O*) Scatter plots represent the proportion of PMN-MDSCs in breast cancer tissue (left) and circulation (right). n=6 per group. Data are presented as mean ± SEM, P values are calculated by Student's t test. **P* <0.05; ***P* <0.01; ****P* <0.001.

Table S1: Clinical information of 61 female breast cancer patients.

[Seen in Excel file]

Table S2: Clinical information of 163 female breast cancer patients and 18 benign breast tumor patients.

[Seen in Excel file]

Table S3. The description of gene and according enzymes involved in the BCAA biosynthesis pathway.

Gene name	Enzyme	Pathway
*ilv*A	L-threonine dehydratase/deaminase	Isoleucine biosynthesis
*ilv*BN	acetolactate (acetohydroxyacid) synthase	Leucine, Isoleucine and Valine biosynthesis
*ilv*C	keto acid isomeroreductase	Leucine, Isoleucine and Valine biosynthesis
*ilv*D	dihydroxyacid dehydratase	Leucine, Isoleucine and Valine biosynthesis
*ilv*E	branched-chain aminotransferase	Leucine, Isoleucine and Valine biosynthesis
*leu*A	isopropylmalate synthase	Leuince biosynthesis
*leu*B	isopropylmalate isomerase	Leuince biosynthesis
*leu*CD	isopropylmalate dehydrogenase	Leuince biosynthesis

Table S4. The information of presence of BCAA biosynthesis related genes in differential microbiota.

Change	Differential texas	Present	Absent
Increase in overweight/obese patients or HFD mice	g: Eubacterium_coprostanoligenes (human)	*ilv*A *ilv*B *ilv*C *ilv*D *ilv*E *leu*A *leu*B *leu*CD	
	g: Desulfovibrio (human & mice)	*ilv*A *ilv*B *ilv*C *ilv*D *ilv*E *leu*A *leu*B *leu*CD	
	g: Blautia (mice)	*ilv*A *ilv*B *ilv*C *ilv*D *ilv*E *leu*A *leu*B *leu*CD	
	g:Ruminiclostridium (mice)	*ilv*B *ilv*C *ilv*D *ilv*E *leu*A *leu*B *leu*CD	*ilv*A
	g: Faecalimonas (human)	*ilv*A *ilv*B *ilv*C *ilv*D *ilv*E *leu*A *leu*B *leu*CD	
Decrease in overweight/obese patients or HFD mice	g: Gemella (human)	*ilv*A *ilv*B *ilv*E *leu*B *leu*CD	*ilv*C *ilv*D *leu*A
	g: Solobacterium (human)		*ilv*A *ilv*B *ilv*C *ilv*D *ilv*E *leu*A *leu*B *leu*CD
	g: Alloprevotella (mice)	*ilv*A *ilv*B *ilv*D *ilv*E	*ilv*C *leu*A *leu*B *leu*CD

Table S5. Antibody infromation

Antibody	Company	Cat.
Ki67	Cell Signaling Technology	12202
APC-Cy7-Viability Dye	Invitrogen	65-0865-18
V450- Viability Dye	Invitrogen	65-0863-18
BV421-Anti-CD45	Biolegend	103133
Percp/Cy5.5-Anti-CD3	Biolegend	100327
BV510-Anti-CD4	Biolegend	100449
BV-421-Anti-CD8	Biolegend	100737
FITC-Anti-CD4	Invitrogen	88-8118-40
PE-Anti-CD25	Invitrogen	88-8118-40
APC-Anti-Foxp3	Invitrogen	88-8118-40
PE-Anti-NK1.1	Biolegend	108707
APC-Anti-CD11b	Biolegend	101211
PE-Anti-F4/80	Biolegend	123110
FITC-Anti-CD11c	Biolegend	117306
Percp/Cy5.50-Anti-CD206	Biolegend	141716
Percp/Cy5.5-Anti-Gr-1	Biolegend	127615
PE/Cy7-Anti-Ly-6C	Biolegend	128018
FITC-Anti-Ly-6G	BD Pharmingen	551460
PE/Cy7-Anti-CD11c	Biolegend	117318
PE/Cy7 Anti--Ki67	Biolegend	652426
PE-Anti-CXCR2	Biolegend	149304
V450-Anti-Lineage	Invitrogen	88-7772-72
Percp/Cy5.5-Anti-Ckit	BD Pharmingen	560557
APC-Anti-SCA-1	Biolegend	108111
FITC-FcγR	Biolegend	101305

Antibody	Company	Cat.
PE-CD34	BD bioscience	128609
Rabbit CD3e antibody	Abcam	AB16669
Mouse CD33 antibody	R&D	MAB11371
Eflour488-Linked Goat Anti-Rabbit Antibody	Invitrogen	A-11008
CFSE	Invitrogen	C34554
In Vivo Anti-Gr-1	Bioxcell	BP0075
mTOR antibody	Cell Signaling Technology	2972
Phospho- mTOR(Ser2448) antibody	Cell Signaling Technology	5536
P70S6k antibody	Cell Signaling Technology	2708
Phospho- P70S6k(Thr389) antibody	Cell Signaling Technology	9209
HRP Linked anti-GAPDH	Proteintech	HRP-60004
HRP-linked anti-rabbit IgG	Cell Signaling Technology	7074

Reference

1. Su, S.; Liu, Q.; Chen, J.; Chen, J.; Chen, F.; He, C.; Huang, D.; Wu, W.; Lin, L.; Huang, W.; Zhang, J.; Cui, X.; Zheng, F.; Li, H.; Yao, H.; Su, F.; Song, E., A positive feedback loop between mesenchymal-like cancer cells and macrophages is essential to breast cancer metastasis. (1878-3686 (Electronic)).